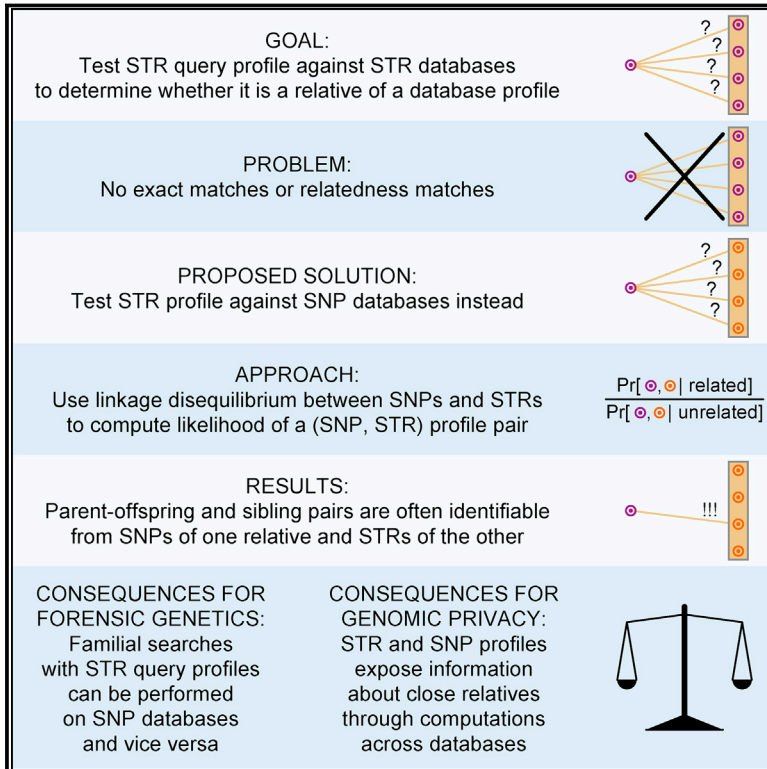# Cell

Statistical Detection of Relatives Typed with Disjoint Forensic and Biomedical Loci

Graphical Abstract

Authors

Jaehee Kim, Michael D. Edge,
Bridget F.B. Algee-Hewitt, Jun Z. Li,
Noah A. Rosenberg

Correspondence

noahr@stanford.edu

In Brief

Genetic data from databases that use nonoverlapping marker sets, such as forensic genetic databases and biomedical and genealogical databases, can be used to connect close relatives, with implications for forensic genetics and genomic privacy.

Highlights

- STR and SNP profiles are tested for relatedness using linkage disequilibrium

- Relatedness can often be detected from SNPs of one relative and STRs of another

- Forensic profiling can seek relatives in databases with nonoverlapping markers

- Genomic privacy of close relatives is affected by cross-database computations

CellPress

Statistical Detection of Relatives Typed with Disjoint Forensic and Biomedical Loci

Jaehee Kim,[1] Michael D. Edge,[2] Bridget F.B. Algee-Hewitt,[1] Jun Z. Li,[3] and Noah A. Rosenberg[1,4,*]

[1]Department of Biology, Stanford University, Stanford, CA 94305, USA
[2]Department of Evolution and Ecology, University of California, Davis, Davis, CA 95616, USA
[3]Department of Human Genetics, University of Michigan, Ann Arbor, MI 48109, USA
[4]Lead Contact
*Correspondence: noahr@stanford.edu
 https://doi.org/10.1016/j.cell.2018.09.008

SUMMARY

In familial searching in forensic genetics, a query DNA profile is tested against a database to determine whether it represents a relative of a database entrant. We examine the potential for using linkage disequilibrium to identify pairs of profiles as belonging to relatives when the query and database rely on nonoverlapping genetic markers. Considering data on individuals genotyped with both microsatellites used in forensic applications and genome-wide SNPs, we find that ∼30%–32% of parent-offspring pairs and ∼35%–36% of sib pairs can be identified from the SNPs of one member of the pair and the microsatellites of the other. The method suggests the possibility of performing familial searches of microsatellite databases using query SNP profiles, or vice versa. It also reveals that privacy concerns arising from computations across multiple databases that share no genetic markers in common entail risks, not only for database entrants, but for their close relatives as well.

INTRODUCTION

Forensic DNA testing sometimes seeks to identify unknown individuals through familial searching, or relatedness profiling. When no exact match of a query DNA profile to a database of profiles is found, investigators can potentially test for a partial match to determine whether the query profile might instead represent a close relative of a person whose profile appears in the database (Bieber et al., 2006; Gershaw et al., 2011; Butler, 2012). A positive test leads investigators to consider relatives of the person with the partial match as possible contributors of the query profile.

Familial searching expands the potential to identify unknown contributors beyond the level achieved when searching exclusively for exact database matches. The larger set of people accessible to investigators—database entrants, plus their relatives—can increase the probability that the true contributor of a query profile is identified (Bieber et al., 2006; Curran and Buckleton, 2008). However, the accessibility of relatives to investigators

in database queries raises privacy and legal policy concerns, as considerations guiding appropriate inclusion of DNA profiles in databases and subsequent use of those profiles generally focus on the contributors of the profiles rather than on close relatives who are rendered accessible to investigators (Greely et al., 2006; Murphy, 2010). Concerns about privacy vary in magnitude across populations, as false-positive identifications of relatives might be substantially more likely to affect members of populations with lower genetic diversity, and hence a greater likelihood of chance partial matches (Rohlfs et al., 2012, 2013), or members of populations overrepresented in DNA databases (Greely et al., 2006; Chow-White and Duster, 2011).

Recently, considering genome-wide single-nucleotide polymorphisms (SNPs) together with the Combined DNA Index System (CODIS) microsatellite markers used for forensic genetic databases in the United States and elsewhere (Budowle et al., 2001; Butler, 2006; Hares, 2015), we studied the possibility of matching a forensic-genetic record in one database to a profile on a set of nonoverlapping genetic markers in a different database. We showed that records could be matched between databases with no overlapping genetic markers, provided that sufficiently strong linkage disequilibrium (LD) exists between markers appearing in the two databases (Edge et al., 2017). The approach could facilitate development of new SNP-based forensic marker systems that are backward-compatible with the CODIS microsatellites, as it could enable a query SNP profile to be tested for a match to a microsatellite database or vice versa. It also uncovers privacy concerns, as an individual present in a SNP database—collected in a biomedical, genealogical, or personal genomics setting, for example—might be possible to link to a CODIS profile, and vice versa, in a manner not intended in the context of either database examined in isolation. First, a SNP database entrant could become accessible to forensic investigation. Second, although in the United States, the use of forensic genetic markers given protections against unreasonable searches is based partly on a premise that these markers provide only the capacity for identification and do not expose phenotypic information (Greely and Kaye, 2013; Katsanis and Wagner, 2013; United States Supreme Court, 2013), phenotypes that are possible to predict from a SNP profile could potentially be predicted from a CODIS profile by connecting the CODIS profile to a SNP profile and then predicting phenotypes from the SNPs.

Does cross-database record matching extend to relatives? In other words, is it possible to identify a genotype record with one

Table 1. The Joint Distribution of the Cotterman Identity State C_k and the Genotype $R_{B\ell}$ of Individual B at STR Locus ℓ

Identity state	STR genotype $R_{B\ell}$ of individual B		Marginal probability of identity state C_k
	$a_i a_i$	$a_i a_j, j \neq i$	
C_0	$p_i^2 \Delta_0$	$2 p_i p_j \Delta_0$	Δ_0
C_1	$p_i^2 \Delta_1$	$2 p_i p_j \Delta_1$	Δ_1
C_2	$p_i^2 \Delta_2$	$2 p_i p_j \Delta_2$	Δ_2
Marginal probability of genotype $R_{B\ell}$	p_i^2	$2 p_i p_j$	1

In the three identity states C_0 to C_2 for individuals A and B, the alleles of individuals A and B appear as the top and bottom pairs of dots, respectively. Identical-by-descent alleles are connected by lines. The probability of state C_k is denoted Δ_k, with $\sum_{k=0}^{2} \Delta_k = 1$. Genotypes are unordered, and p_i denotes the frequency of allele a_i. The marginal probability of state C_k, $\mathbb{P}(C_k)$, is obtained by summing over all possible alleles a_i and a_j at the locus, $\sum_{i=1}^{N_\ell} \sum_{j=i}^{N_\ell} \mathbb{P}(R_{B\ell} = a_i a_j, C_k)$, where N_ℓ is the number of distinct alleles at STR locus ℓ. The marginal probability of genotype $R_{B\ell}$, $\mathbb{P}(R_{B\ell})$, is a sum over identity states: $\sum_{k=0}^{2} \mathbb{P}(R_{B\ell}, C_k)$.

set of genetic markers as originating from a relative of the contributor of a genotype record obtained with a distinct, nonoverlapping set of markers? If so, then new marker systems in the forensic context could permit relatedness profiling in a manner that is compatible with existing marker systems, as a profile from a new SNP or DNA sequence system could be tested for relationship matches to existing microsatellite profiles. However, a substantial privacy concern would also be raised, as inclusion in a biomedical, genealogical, or personal genomics dataset could expose relatives of the participant to forensic investigation; moreover, phenotypes of a relative could potentially be identifiable from a forensic profile.

Here, extending the likelihood framework of Edge et al. (2017) to accommodate familial relationships, we devise and evaluate an algorithm for using linkage disequilibrium to perform cross-database matching of relatives. We assess the performance of record matching between SNP profiles and microsatellite profiles gathered with distinct marker sets, in the case in which the SNP profile and the microsatellite profile represent distinct but closely related individuals. The results contribute to the evaluation of the genetic privacy of existing forensic marker systems, as well as to assessment of the potential of familial searching with new SNP or DNA sequence marker systems that might be devised in the future.

RESULTS

Likelihood Method

We consider a dataset that contains L microsatellites, or short-tandem-repeat (STR) loci, each surrounded by an associated

set of neighboring SNPs. For two individuals A and B, we denote by $R_{A\ell}$ the diploid genotype of individual A at STR locus ℓ and by $S_{B\ell}$ the set of diploid genotypes of individual B at the neighboring SNP loci associated with STR locus ℓ. Considering all L STR loci, we let R_A be the STR profile of individual A from the STR dataset, $R_A = \{R_{A1}, R_{A2}, \ldots, R_{AL}\}$, and we let S_B be the SNP profile of individual B from the SNP dataset, $S_B = \{S_{B1}, S_{B2}, \ldots, S_{BL}\}$.

We characterize the familial relationship between two individuals A and B by the three Cotterman identity coefficients, Δ_0, Δ_1, and Δ_2, respectively representing the probabilities of three identity states C_0, C_1, and C_2 (Jacquard, 1972; Lange, 1997). Each Δ_k represents the probability that two diploid individuals share k alleles identically by descent at an autosomal locus (Table 1).

We test a hypothesis that A and B, assumed to be non-inbred, are related with a relationship defined by an identity coefficient vector, $\mathbf{\Delta} = (\Delta_0, \Delta_1, \Delta_2)$, against the null hypothesis in which the two individuals are unrelated. To test the hypothesis, we generalize the log-likelihood-ratio match score of Edge et al. (2017):

$$\lambda(R_A, S_B) = \ln[\mathbb{P}(R_A \mid S_B, M = \mathbf{\Delta})] - \ln[\mathbb{P}(R_A)], \quad \text{(Equation 1)}$$

where M is a variable indicating the hypothesized relationship between individuals A and B. Edge et al. (2017) assumed that M represented the hypothesis in which A and B are the same individual; we consider relationship hypotheses more generally. As the natural logarithm of a likelihood ratio, a match score of 10, for example, represents a value of $e^{10} \approx 22,026$ for the ratio $\mathbb{P}(R_A \mid S_B, M = \mathbf{\Delta})/\mathbb{P}(R_A)$.

Assuming independence of the STR loci, so that genotypes at separate STRs are independent, we can rewrite Equation 1 as a sum of log-likelihood ratios across STR loci:

$$\lambda(R_A, S_B) = \sum_{\ell=1}^{L} [\ln[\mathbb{P}(R_{A\ell} \mid S_{B\ell}, M = \mathbf{\Delta})] - \ln[\mathbb{P}(R_{A\ell})]].$$

(Equation 2)

The likelihood $\mathbb{P}(R_{A\ell} \mid S_{B\ell}, M = \mathbf{\Delta})$ for arbitrary hypotheses $\mathbf{\Delta}$ for the relationship between A and B is obtained by a decomposition over possible values of $R_{B\ell}$, the STR genotype of B. The decomposition, which provides the methodological advance beyond Edge et al. (2017), considers products of terms $\mathbb{P}(R_{A\ell} \mid R_{B\ell}, \mathbf{\Delta})$ reflecting the relationship of A and B, and terms $\mathbb{P}(R_{B\ell} \mid S_{B\ell})$, reflecting STR genotype probabilities conditional on surrounding SNP probabilities. Details appear in the STAR Methods (Overview of Match Score Calculation).

Experimental Design

To perform cross-database matching of relatives, we begin from datasets with N_R STR and N_S SNP profiles, where some or all of the profiles in one dataset represent relatives of individuals whose profiles appear in the other dataset. For each pair of profiles (R_A, S_B), one from each dataset, we compute the match score $\lambda(R_A, S_B)$ under a specified hypothesis for the relationship $\mathbf{\Delta}$ between the pair. The match-score matrix $\mathbf{X}$ is an $N_S \times N_R$ matrix whose (i, j) entry is $\lambda(i, j)$. From the match-score matrix, we identify matches according to each of four match-assignment algorithms. For simplicity, we assume $N_R = N_S$.
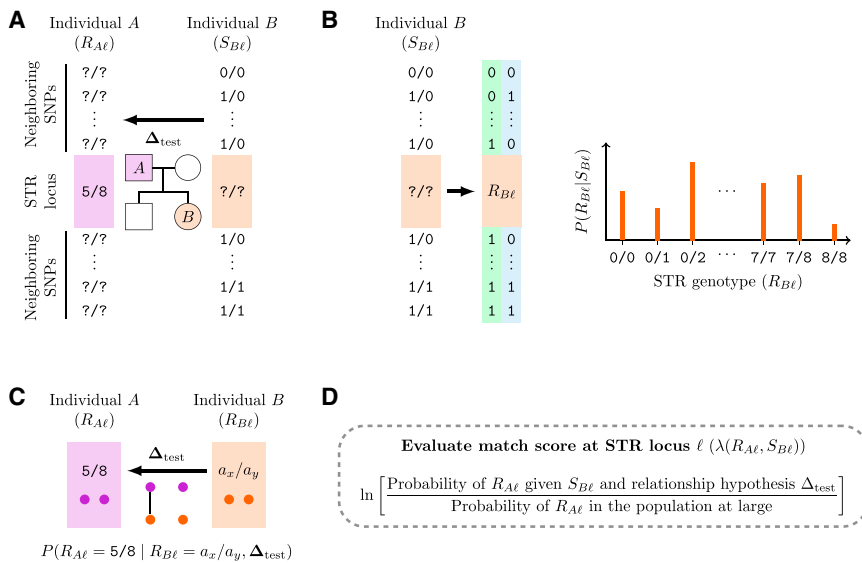
A

Individual A ($R_{A\ell}$)   Individual B ($S_{B\ell}$)

Neighboring SNPs

?/?   0/0
?/?   1/0
⋮   ⋮
?/? Δ_{test} 1/0

STR locus

5/8   ?/?

Neighboring SNPs

?/?   1/0
⋮   ⋮
?/?   1/1
?/?   1/1

B

Individual B ($S_{B\ell}$)

0/0   0 0
1/0   0 1
⋮   ⋮ ⋮
1/0   1 0

?/? → $R_{B\ell}$

1/0   1 0
⋮   ⋮ ⋮
1/1   1 1
1/1   1 1

$P(R_{B\ell}|S_{B\ell})$

STR genotype ($R_{B\ell}$)

0/0 0/1 0/2 ⋯ 7/7 7/8 8/8

C

Individual A ($R_{A\ell}$)   Individual B ($R_{B\ell}$)

5/8 Δ_{test} a_x/a_y

$P(R_{A\ell} = 5/8 \mid R_{B\ell} = a_x/a_y, \mathbf{\Delta}_{\text{test}})$

D

Evaluate match score at STR locus ℓ ($\lambda(R_{A\ell}, S_{B\ell})$)

$$\ln\left[\frac{\text{Probability of } R_{A\ell} \text{ given } S_{B\ell} \text{ and relationship hypothesis } \mathbf{\Delta}_{\text{test}}}{\text{Probability of } R_{A\ell} \text{ in the population at large}}\right]$$

Figure 1. Schematic for Evaluating $\lambda(R_A, S_B)$, the Match Score for a Pairing of STR Profile R_A of Individual A and SNP Profile S_B of Individual B, Assuming a Relationship Hypothesis $\mathbf{\Delta}_{\text{test}}$ between Individuals A and B

Because the match score is a sum of contributions from L STR loci (Equation 2), we illustrate steps for computing the match score $\lambda(R_{A\ell}, S_{B\ell})$ of a single locus ℓ.

(A) The data and the hypothesis tested. Consider individual A with unordered diploid STR genotype $R_{A\ell} = 5/8$ and individual B with SNP profile $S_{B\ell}$ around locus ℓ. We seek to test a hypothesis that A is a parent of B.

(B) Imputation of the STR in individual B. Given the SNP profile $S_{B\ell}$ of individual B, we use BEAGLE to estimate the STR genotype probabilities $\mathbb{P}(R_{B\ell} \mid S_{B\ell})$ using a phased training set as a reference panel.

(C) Conditional probability of the STR genotype of A given the probabilistically imputed STR genotype of B and a test hypothesis $\mathbf{\Delta}_{\text{test}}$. Under the hypothesis $\mathbf{\Delta}_{\text{test}}$, considering all condensed identity states possible for a pair of individuals given $\mathbf{\Delta}_{\text{test}}$, we compute the probability that individual A has the known STR genotype 5/8 conditional on the imputed STR genotype a_x/a_y: $\mathbb{P}(R_{A\ell} = 5/8 \mid R_{B\ell} = a_x/a_y, \mathbf{\Delta}_{\text{test}})$. We evaluate this probability for all STR genotypes possible for individual B.

(D) The match score at locus ℓ. Multiplying terms $\mathbb{P}(R_{B\ell} \mid S_{B\ell})$ from (B) and $\mathbb{P}(R_{A\ell}|R_{B\ell}, \mathbf{\Delta}_{\text{test}})$ from (C) and summing over all possible STR genotypes $R_{B\ell}$ of B at locus ℓ (Equation 5), we obtain $\mathbb{P}(R_{A\ell} \mid S_{B\ell}, \mathbf{\Delta}_{\text{test}})$, the probability of the STR genotype of individual A at locus ℓ given the SNP genotype of individual B around locus ℓ and the relationship hypothesis. The match score of locus ℓ (the summand in Equation 2) is expressed as a log-likelihood ratio of the test hypothesis $\mathbf{\Delta}_{\text{test}}$ and the null hypothesis that A and B are unrelated. The match scores we use, relying on natural logarithms, can be converted to base-10 logarithms by dividing by $\ln 10 \approx 2.30$, so that a 1,000:1 ratio has match score 6.91 with base e and 3 with base 10.

Relationship Schemes

We used datasets containing genotypes at 13 STR loci and 642,563 SNP loci in 872 Human Genome Diversity Panel individuals (STAR Methods, Experimental Model and Subject Details). Although our approach applies for arbitrary relationship hypotheses, we focused on close relationships, for which SNPs of one individual in a relative pair are most likely to contain information about STRs of the other and vice versa. Assuming that individuals were not inbred, we considered three schemes for $\mathbf{\Delta}_{\text{true}}$, the true relationship between individuals in the STR and SNP datasets: (1) same individual, $\mathbf{\Delta}_{\text{true}} = (0, 0, 1)$; (2) parent-offspring, $\mathbf{\Delta}_{\text{true}} = (0, 1, 0)$; and (3) sibling pairs, $\mathbf{\Delta}_{\text{true}} = (1/4, 1/2, 1/4)$. For schemes 2 and 3, we simulated pedigrees based on the actual genotype data to produce datasets containing relatives (STAR Methods, Pedigree Generation).

Following Edge et al. (2017), for each scheme for the true relationship between individuals in the STR and SNP datasets, we generated 100 random partitions of the individuals into a training set (75%) and a test set (25%) (STAR Methods, Training and Test Sets). For each partition, using BEAGLE (Browning and Browning, 2007, 2016), we phased the training set to produce haplotypes containing STR loci and their surrounding SNPs (STAR Methods, BEAGLE Settings). Next, as in Edge et al. (2017), we used the phased training set as a reference and augmented it with the SNP genotypes of the unphased test set. We then used BEAGLE to impute STR genotypes in the test set based on the neighboring SNPs (STAR Methods, Training and Test Sets).

Once STR genotype probabilities for individuals in the SNP dataset were obtained by imputation, we computed the match score (Equation 2) for all possible pairs of individuals, one in the SNP dataset and one in the STR dataset, under three relationship hypotheses: (1) same individual, (2) parent-offspring, and (3) sib pairs. Letting $\mathbf{\Delta}_{\text{test}}$ denote the hypothesized relationship from which we computed the match score, we considered nine choices for the pair ($\mathbf{\Delta}_{\text{true}}, \mathbf{\Delta}_{\text{test}}$). A schematic of the computation appears in Figure 1.

When the relationship hypothesis tested and the true relationship are the same ($\mathbf{\Delta}_{\text{true}} = \mathbf{\Delta}_{\text{test}}$), diagonal entries in the match-score matrix $\mathbf{X}$ represent match scores for true relationship matches, and off-diagonal entries give match scores for unrelated individuals. When $\mathbf{\Delta}_{\text{true}} \neq \mathbf{\Delta}_{\text{test}}$, however, the model is misspecified; in this case, a diagonal entry gives the match score for the test hypothesis when two individuals are related but the relationship hypothesis tested differs from the true relationship. An off-diagonal entry gives the match score for the test hypothesis for unrelated individuals.

Match-Assignment Scenarios

Given a match-score matrix $\mathbf{X}$ for the pair ($\mathbf{\Delta}_{\text{true}}, \mathbf{\Delta}_{\text{test}}$), we considered four matching scenarios: one-to-one matching, one-to-many matching with a query SNP profile, one-to-many matching with a query STR profile, and needle-in-haystack matching (Edge et al., 2017). In one-to-one matching, we assume that it is already known that each profile in the SNP dataset has exactly one true relative in the STR dataset and vice versa. To find the pairing of profiles that maximizes the sum of match scores across all paired profiles, we use the Hungarian algorithm (Kuhn, 1955) as in Edge et al. (2017). Record-matching accuracy is the fraction of pairs correctly matched.

In one-to-many matching, we relax the one-to-one correspondence and examine the possibility that an observation in one
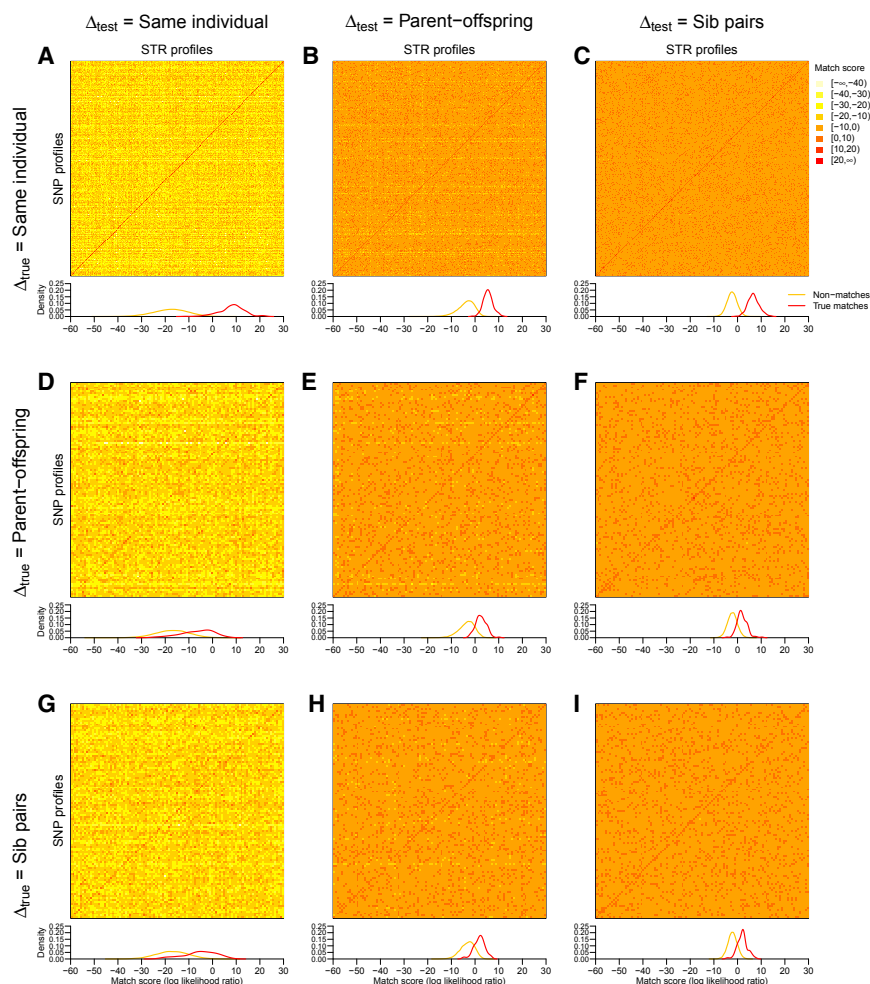
Figure 2. Match Scores of SNP and STR Profiles in Various Relatedness Settings

Δ_{true} denotes a true relationship between pairs of individuals represented on the diagonal of a matrix, one from a SNP dataset and the other from an STR dataset. Δ_{test} represents a test relationship hypothesis from which match scores are computed. Of 100 random partitions of individuals into training and test sets, the results from the partition with median one-to-one record-matching accuracy are shown. For each $(\Delta_{true}, \Delta_{test})$ scheme, we plot the match-score matrix (top) and the kernel density estimate for match scores (bottom). The kernel density estimates separately consider the diagonal entries (true matches) and the off-diagonal entries (non-matches).

(A) Δ_{true}, same individual; Δ_{test}, same individual.
(B) Δ_{true}, same individual; Δ_{test}, parent-offspring.
(C) Δ_{true}, same individual; Δ_{test}, sib pairs.
(D) Δ_{true}, parent-offspring; Δ_{test}, same individual.
(E) Δ_{true}, parent-offspring; Δ_{test}, parent-offspring.
(F) Δ_{true}, parent-offspring; Δ_{test}, sib pairs.
(G) Δ_{true}, sib pairs; Δ_{test}, same individual.
(H) Δ_{true}, sib pairs; Δ_{test}, parent-offspring.
(I) Δ_{true}, sib pairs; Δ_{test}, sib pairs.

score across all non-matching pairs. This stringent criterion identifies as matches only those pairs with the highest match scores.

Record-Matching Accuracy

For each of the three choices of Δ_{true}, we considered 100 partitions of the initial sample into a training set and a test set (STAR Methods, Training and Test Sets). For each of the three test hypotheses Δ_{test}, we then computed the match score (Equation 2) for all pairs of profiles in the test set, one from the STR dataset and one from the SNP dataset. For each pair $(\Delta_{true}, \Delta_{test})$, the match-score matrix corresponding to the median record-matching accuracy across 100 partitions in one-to-one matching appears in Figure 2, along with the associated distributions of match scores for true matches and non-matches. Table 2 presents the median, minimum, and maximum accuracies.

When $\Delta_{test} = (0, 0, 1)$, our generalized match score in Equation 2 is equivalent to that of Edge et al. (2017) for identifying the same individual in two disjoint datasets. Our results under the setting $\Delta_{true} = \Delta_{test} = (0, 0, 1)$ closely follow Edge et al. (2017). Most match scores for true matches exceed most match scores for non-matches, so that the diagonal entries of the match-score matrix have generally larger values than off-diagonal entries (Figure 2A). In one-to-one matching, among 100 partitions into the training and test sets, the median record-matching accuracy is 214 of 218 (98.2%).

With $\Delta_{true} = \Delta_{test} = (0, 1, 0)$, we search for parent-offspring relationships between a SNP profile and an STR profile. Match scores for true relationship matches also generally exceed those for non-matches, so the distribution of diagonal entries is shifted

dataset might be identified as having multiple relationship matches in another dataset. In the case in which a SNP profile is used as a "query," for a given SNP profile, the STR profile with the largest match score is proposed as its match. In other words, for each row of the match-score matrix, we select the largest entry in the row. Record-matching accuracy is the fraction of SNP profiles matched to the correct STR profiles. In this scenario, a SNP profile has exactly one putative STR profile, but an STR profile can be chosen as the match for multiple SNP profiles. Similarly, in one-to-many matching with an STR profile as the query, we select the SNP profile with the largest match score for the given STR profile: for each column of the match-score matrix, the largest entry is chosen as a match. Record-matching accuracy is the fraction of STR profiles matched to the correct SNP profiles.

In needle-in-haystack matching, unlike in the other scenarios, we investigate a setting in which a database query is performed for only one profile. A perfect matching is achieved when no overlap occurs in the match-score distributions of the correct relationship matches and the incorrect matches. We quantified the record-matching accuracy as the proportion of true relatedness matches with greater match scores than the largest match

Table 2. Record-Matching Accuracies between Genome-wide SNP and CODIS STR Profiles

Δ_{true} ╲ Δ_{test}	Same Individual		Parent-Offspring		Sib Pairs		Match-Assignment Scenario
	Median	Min, Max	Median	Min, Max	Median	Min, Max	
Same individual	0.982	0.917, 1.000	0.885	0.807, 0.982	0.968	0.908, 1.000	one-to-one
	0.908	0.862, 0.950	0.780	0.716, 0.858	0.878	0.830, 0.927	one-to-many: SNP query
	0.904	0.830, 0.945	0.780	0.716, 0.844	0.688	0.596, 0.748	one-to-many: STR query
	0.431	0.064, 0.697	0.085	0.000, 0.294	0.202	0.018, 0.440	needle-in-haystack
Parent-offspring	0.174	0.101, 0.257	0.312	0.239, 0.440	0.266	0.165, 0.367	one-to-one
	0.183	0.083, 0.266	0.303	0.229, 0.422	0.266	0.183, 0.330	one-to-many: SNP query
	0.165	0.064, 0.239	0.321	0.220, 0.385	0.275	0.174, 0.358	one-to-many: STR query
	0.000	0.000, 0.055	0.018	0.000, 0.092	0.018	0.000, 0.092	needle-in-haystack
Sib pairs	0.294	0.165, 0.450	0.303	0.174, 0.431	0.349	0.229, 0.459	one-to-one
	0.284	0.220, 0.367	0.303	0.211, 0.394	0.349	0.248, 0.459	one-to-many: SNP query
	0.275	0.183, 0.358	0.303	0.211, 0.413	0.358	0.257, 0.450	one-to-many: STR query
	0.028	0.000, 0.110	0.028	0.000, 0.119	0.046	0.000, 0.119	needle-in-haystack

For each of three choices for the true relationship between corresponding profiles in the SNP and STR datasets (Δ_{true}) and for each of three choices for the relationship hypothesis tested (Δ_{test}), in each of four match-assignment scenarios (one-to-one, one-to-many with a query SNP profile, one-to-many with a query STR profile, and needle-in-haystack), the minimum, median, and maximum accuracies across 100 partitions of the sample into a training set (75%) and test set (25%) are shown. For $\Delta_{true} = \Delta_{test}$ (block-diagonal entries), each entry shows the fraction of individuals correctly matched to their true relatives. For $\Delta_{true} \neq \Delta_{test}$, each entry represents the fraction of individuals matched to their true relatives under a misspecified relationship hypothesis Δ_{test}. See Tables S1 and S2 for corresponding analyses with 17-STR and 20-STR marker sets, and Table S3 for an analysis that considers ancestry information. An analysis of the partitions underlying the table with an expanded set of relationship hypotheses appears in Figure S1.

toward higher values compared to the distribution of off-diagonal entries (Figure 2E). The distinction between diagonal and off-diagonal entries is not as great as when profiles represent the same individual rather than parent-offspring pairs. The median record-matching accuracy for one-to-one matching is 31.2% (34 of 109 individuals).

The case of sib-pair relationships between SNP and STR profiles, $\Delta_{true} = \Delta_{test} = (1/4, 1/2, 1/4)$ (Figure 2I), is similar to the case of parent-offspring relationships. Diagonal and off-diagonal match-score matrix entries are differentiated, though not as strongly as in matching profiles from the same individual. The median record-matching accuracy for one-to-one matching is 34.9% (38 of 109 individuals).

Model Misspecification

Considering the six ($\Delta_{true}, \Delta_{test}$) pairs with $\Delta_{true} \neq \Delta_{test}$, we observe that record-matching accuracies for misspecified test hypotheses are generally lower than in corresponding cases with the test hypothesis correctly specified (Figure 2; Table 2). The value of Δ_{true} has a stronger influence on record-matching than does Δ_{test}; for example, higher accuracies are seen when SNP and STR profiles truly represent the same individual and the test hypothesis is misspecified to search for relative pairs, compared with lower accuracies when profiles represent relatives and the test hypothesis is misspecified to search for exact matches.

For $\Delta_{true} = (0, 0, 1)$, compared to 98.2% median accuracy when $\Delta_{true} = \Delta_{test}$, median accuracy is 88.5% when parent-offspring matches are sought instead of exact matches and 96.8% when sib-pair matches are sought. For $\Delta_{true} = (0, 1, 0)$, compared to 31.2% median accuracy when $\Delta_{true} = \Delta_{test}$, median accuracy is 17.4% for the exact-match test hypothesis and 26.6% for the sib-pair test hypothesis. For $\Delta_{true} = (1/4, 1/2, 1/4)$, compared to 34.9% median accuracy

when $\Delta_{true} = \Delta_{test}$, median accuracy is 29.4% when seeking exact matches and 30.3% when seeking parent-offspring matches.

Match-Assignment Threshold

The number of false-positive matches can be decreased by setting a minimum match-score threshold below which records are left unpaired. This threshold represents a minimum level of stringency specified for identification of matches. For each of the four match-assignment scenarios, the proportions of correct, incorrect, and unassigned profiles with a varying threshold appear in Figure 3 for the partitions with the minimum, median, and maximum record-matching accuracies.

When $\Delta_{true} = \Delta_{test} = (0, 0, 1)$, in the median-accuracy partition in one-to-one matching, as the threshold is decreased, 164 of 218 (75.2%) profiles are correctly matched before an incorrect match is made (top left plot in Figure 3A). The corresponding values are 113 (51.8%) for the minimum-accuracy partition and 218 (100%) for the maximum-accuracy partition. With a decreasing threshold, the minimum-, median-, and maximum-accuracy partitions accurately match 106 (48.6%), 126 (57.8%), and 149 (68.3%) of 218 query SNP profiles (top right plot in Figure 3A), and 112 (51.4%), 154 (70.6%), and 184 (84.4%) of 218 query STR profiles (bottom left plot in Figure 3A), respectively, before an incorrect assignment occurs. In needle-in-haystack matching, in which all matches are incorrect after the first incorrect match, the median partition has 43.1% (94 of 218) accuracy (bottom right plot in Figure 3A). The minimum and maximum accuracies are 6.4% (14 of 218) and 69.7% (152 of 218), respectively.

For the parent-offspring case $\Delta_{true} = \Delta_{test} = (0, 1, 0)$, few pairs are correctly matched before the first incorrect match (Figure 3E). With a threshold that permits false-positives, however, many
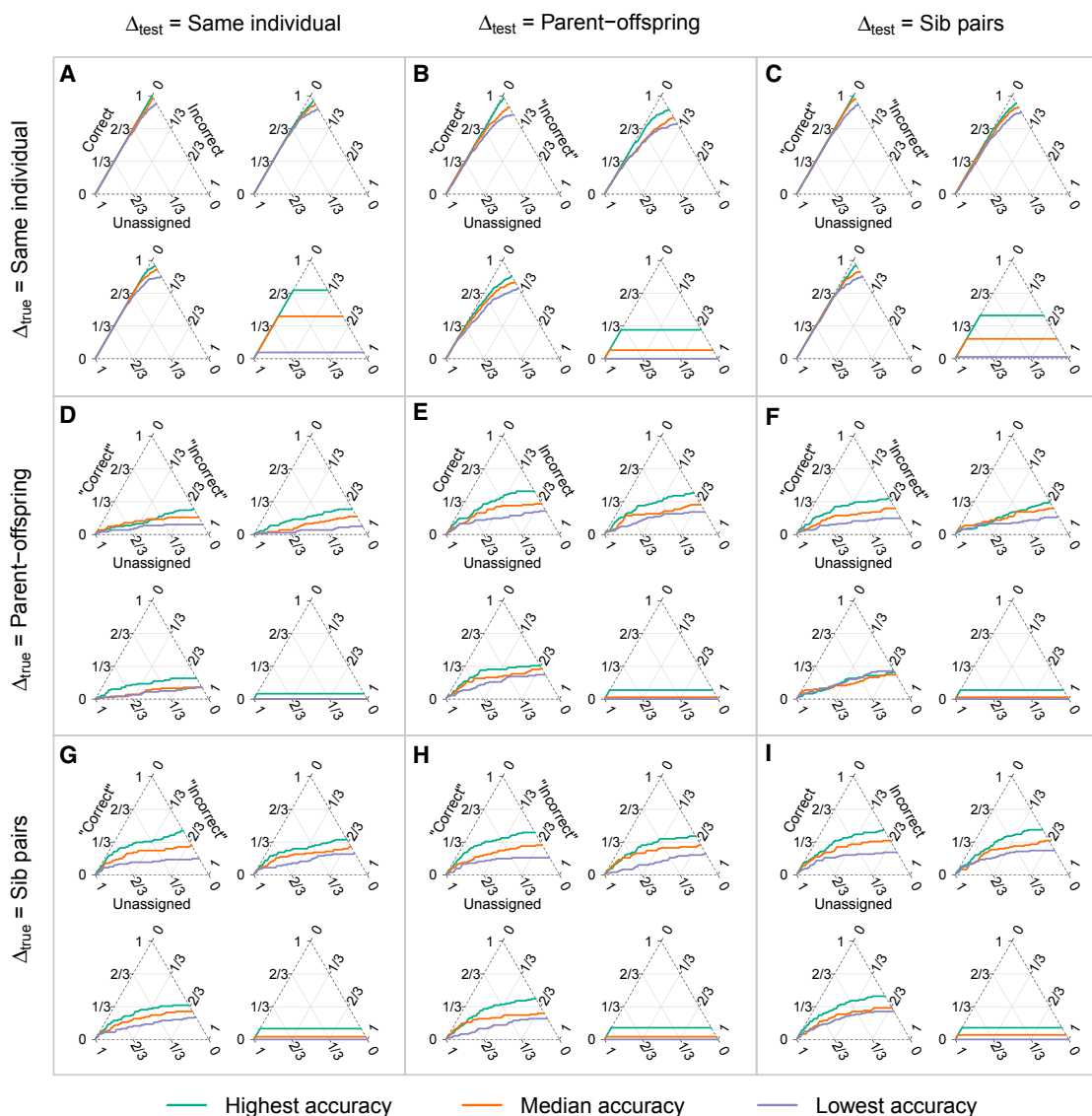
Figure 3. Proportions of Profiles Correctly Assigned, Incorrectly Assigned, and Unassigned with a Varying Match-Score Threshold

For each group of four plots, four match-assignment scenarios are shown: one-to-one matching (top left), one-to-many matching querying a SNP profile and selecting an STR profile with the highest match score (top right), one-to-one matching querying an STR profile and selecting a SNP profile with the highest match score (bottom left), and needle-in-haystack matching, counting the proportion of true matches with match scores exceeding the match scores of all non-matching pairs (bottom right). In each triangle, when the threshold is large, all profiles are unassigned (lower left vertex). Lowering the threshold leads to assignment of all profiles, tracing a curve to the right edge of the triangle. In needle-in-haystack matching, all putative matches have greater match scores than all putative non-matches; thus, once the match-score threshold falls below the largest match score among true non-matches, the number of correct matches remains constant, and the number of incorrect assignments increases while the number of unassigned profiles decreases. For each match-assignment scenario, we plot results from partitions with the minimum, median, and maximum record-matching accuracy across 100 partitions of the sample into training and test sets.

(A) Δ_{true}, same individual; Δ_{test}, same individual.

(B) Δ_{true}, same individual; Δ_{test}, parent-offspring.

(C) Δ_{true}, same individual; Δ_{test}, sib pairs.

(D) Δ_{true}, parent-offspring; Δ_{test}, same individual.

(E) Δ_{true}, parent-offspring; Δ_{test}, parent-offspring.

(F) Δ_{true}, parent-offspring; Δ_{test}, sib pairs.

(G) Δ_{true}, sib pairs; Δ_{test}, same individual.

(H) Δ_{true}, sib pairs; Δ_{test}, parent-offspring.

(I) Δ_{true}, sib pairs; Δ_{test}, sib pairs. In (A), (E), and (I), $\Delta_{true} = \Delta_{test}$. Correct pairs are matched with their true relationship, and incorrect pairs are unrelated but erroneously matched as related. In (B)–(D) and (F)–(H), $\Delta_{true} \neq \Delta_{test}$. "Correct" pairs are true relatives, but the hypothesized relationship is incorrect; "incorrect" pairs are non-relatives inferred to have the relationship in the test hypothesis.

relative pairs are matched correctly: in one-to-one matching, minimum, median, and maximum accuracy are 26 (23.9%), 34 (31.2%), and 48 (44.0%) of 109 profiles, respectively. In one-to-many matching with a SNP query, these values are 25 (22.9%), 33 (30.3%), and 46 (42.2%) of 109, and they are 24 (22.0%), 35 (32.1%), and 42 (38.5%) of 109 for query STR profiles. Needle-in-haystack matching ranges from a minimum of 0 correct matches to a maximum of 10 (9.2%), with a median of 2 (1.8%).

Similar values to the parent–offspring case are obtained for $\Delta_{true} = \Delta_{test} = (1/4, 1/2, 1/4)$, the sib-pair case (Figure 3I). Although even a stringent threshold produces false-positives, many relationships are identified. In one-to-one matching, minimum, median, and maximum record-matching accuracy are 25 (22.9%), 38 (34.9%), and 50 (45.9%) of 109 profiles, respectively. Corresponding values are 27 (24.8%), 38 (34.9%), and 50 (45.9%) of 109 for one-to-many matching with query SNP profiles, and 28 (25.7%), 39 (35.8%), and 49 (45.0%) of 109 for query STR profiles. For needle-in-haystack matching, the minimum, median, and maximum are 0, 5 (4.6%), and 13 (11.9%) correct matches of 109, respectively.

As was observed in one-to-one matching, comparing corresponding panels within the rows of Figure 3, in one-to-many matching with a query SNP profile, one-to-many matching with a query STR profile, and needle-in-haystack matching, the record-matching accuracy with a misspecified test hypothesis is smaller than that seen with the correctly specified hypothesis (Figures 3B–3D and 3F–3H). Corresponding minimum, median, and maximum accuracies are similar under the misspecified hypothesis, as are the trajectories obtained as the match-score threshold decreases.

Additional STRs

We evaluated the dependence of the record-matching accuracy on the number of STR loci by repeating our analyses with random sets of non-CODIS STRs. For each of the three choices of Δ_{true}, considering the median-accuracy partition depicted in Figures 2A, 2E, and 2I, we examined the record-matching accuracy for 100 randomly chosen sets of L loci, with $L = 5, 10, 15, \ldots, 100$ (STAR Methods, Additional STRs).

For each pair $(\Delta_{true}, \Delta_{test})$ and each of the four match-assignment algorithms, Figure 4 depicts the median record-matching accuracy across the 100 locus sets. A comparison of panels within rows of the figure finds that record-matching accuracy is greater for one-to-one matching than for the two one-to-many matching scenarios, which in turn have higher accuracy than the needle-in-haystack scenario. In all panels, accuracy increases with the number of loci, nearing 100% when examining one-to-one and one-to-many matching with 100 loci, and exceeding 80% for needle-in-haystack matching with $\Delta_{true} = \Delta_{test}$. The comparatively lower accuracy seen with the 13 CODIS loci is a consequence of the relatively small size of the CODIS STR panel rather than a limit of the record matching technique.

Comparing panels within columns, accuracy is greater for SNP and STR profiles in which Δ_{true} represents exact matches (Figure 4A) than in cases with parent-offspring (Figure 4B) and sib-pair (Figure 4C) relationships. The correctly specified hy-

pothesis produces greater accuracy than the two misspecified hypotheses, with the highest accuracy occurring for the same-individual hypothesis for Δ_{test} in the panels of Figure 4A, for the parent-offspring hypothesis in Figure 4B, and for the sib-pair hypothesis in Figure 4C.

DISCUSSION

We have found that not only can STR and SNP records be identified as belonging to the same individual, in many cases, STR and SNP profiles can be identified as belonging to close relatives—even though the profiles have no markers shared in common (Table 2). In one-to-one and one-to-many matching, record-matching accuracies were 30%–32% for identification of parent-offspring pairs and 35%–36% for identification of sib pairs, increasing toward 100% as the number of markers in the STR profile was increased to 100 (Figure 4).

The record-matching accuracies for parent-offspring pairs and sib pairs—relationships with the same overall kinship coefficient—were lower than the accuracies observed for STR and SNP profiles originating from the same individual. Record-matching of profiles from relatives is weakened because STR alleles in one profile of a pair and the neighboring SNP haplotypes in the other profile need not have been co-inherited from the same ancestor.

Interestingly, when the relatedness hypothesis tested was misspecified, the reduction in accuracy was relatively small. Parent-offspring pairs were identified by record matching with a sib-pair hypothesis for the relationship with accuracy 27%–28% for one-to-one and one-to-many matching, and sib pairs were identified with a parent-offspring hypothesis with 30% accuracy (Table 2). Pairs of relatives were also revealed by record matching when searching for exact matches, although with slightly lower accuracies of 17%–18% for parent-offspring pairs and 28%–29% for sib pairs. These results suggest that in practical settings in which the true relationship between profiles of interest to match is unknown, relative pairs will often be identified even when testing an incorrect relationship hypothesis.

This study contributes to a growing body of work on inference of genetic relationships in scenarios more challenging than when relatives are typed for the same markers (Vohr et al., 2015; Snyder-Mackler et al., 2016; Dou et al., 2017; Martin et al., 2017; Theunert et al., 2017; Kuhn et al., 2018). In the setting of ancient DNA, Vohr et al. (2015) focused on the scenario in which DNA sequence data are generated for different DNA samples possibly representing the same or related individuals—from a burial site, for example—but are sufficiently sparse that reads do not necessarily overlap between samples. In a computation centered on detecting samples representing the same individual, Vohr et al. (2015) could distinguish simulated parent-offspring pairs and sib pairs from unrelated pairs; this computation amounts to demonstrating that under a same-individual hypothesis for Δ_{test}, pairs with a parent–offspring or sib relationship for Δ_{true} were uncovered. A second study formally estimating relatedness from sparse sequence data while making use of LD between sites with data available in different sampled individuals was able to identify second- and third-degree relative pairs (Dou et al., 2017). These various studies use forms of genetic
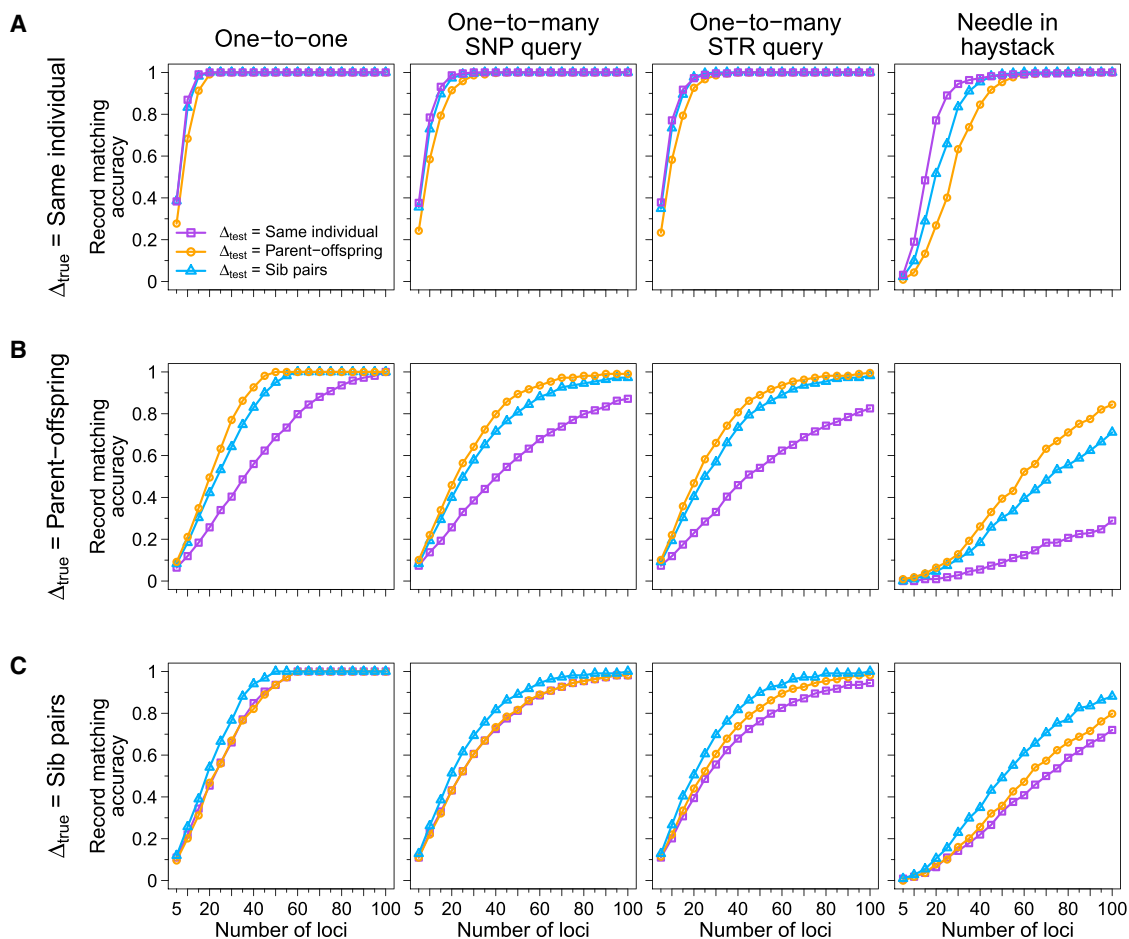
Figure 4. Record-Matching Accuracy as a Function of the Number of STRs

For each number of loci at intervals of 5 loci, 100 random locus sets are analyzed for the data partition in Figure 2.

(A) Δ_{true}, same individual.

(B) Δ_{true}, parent-offspring.

(C) Δ_{true}, sib pairs. In each of the 12 plots representing a choice of Δ_{true} and a match-assignment algorithm, three lines are shown, representing the median record-matching accuracy across 100 loci for each of three choices of Δ_{test}.

data other than STRs and SNPs, highlighting that the potential for record matching with relatives extends in principle to any data types with sufficient LD between marker sets.

The potential to perform familial searching of forensic STR profiles in SNP databases generates both opportunities and privacy risks. Because accuracy was 30%–36% for identification of first-degree relatives rather than above 90% as was seen for paired profiles from the same individuals, identification of relatives by record matching with our one-to-one and one-to-many algorithms will be possible in fewer cases. However, if a match to a particular query STR profile is of interest, an algorithm can be envisioned in which many top SNP database hits are further explored—by additional genotyping of contributors for whom DNA is available or by genealogical tracing of relatives of the contributors to uncover exact matches (Figure 5A). A relaxed accuracy measure in such a setting could therefore tabulate true matches that have high match scores (but not necessarily the highest) or that differ in score from the highest value by less

than a specified constant. Although accuracy with larger marker panels depends on the specific loci considered and such variables as their recombination context, it can increase substantially even with relatively few additional STRs (Figure 4). As of 2017, new CODIS profiles consider 20 markers including the original 13 (Hares, 2015); when we repeat our analysis using the original 13 markers together with 4 markers from the 2017 update, accuracy rates for identification of first-degree relatives increase from 30%–36% to 43%–51% (Table S1), and when we add to the 17 markers sets of 3 random markers to mimic the 20-locus CODIS set, they are 48%–54% (Table S2).

Record matching of pairs of relatives between STR and SNP databases has a significant impact on genetic privacy. In addition to magnifying the exposure of the relatives of SNP-profile contributors to forensic identification, it also increases the phenotypic reach of STR profiles. CODIS genotypes of one individual could potentially be associated with genomic SNP genotypes of a relative, which could, in turn, reveal phenotypes
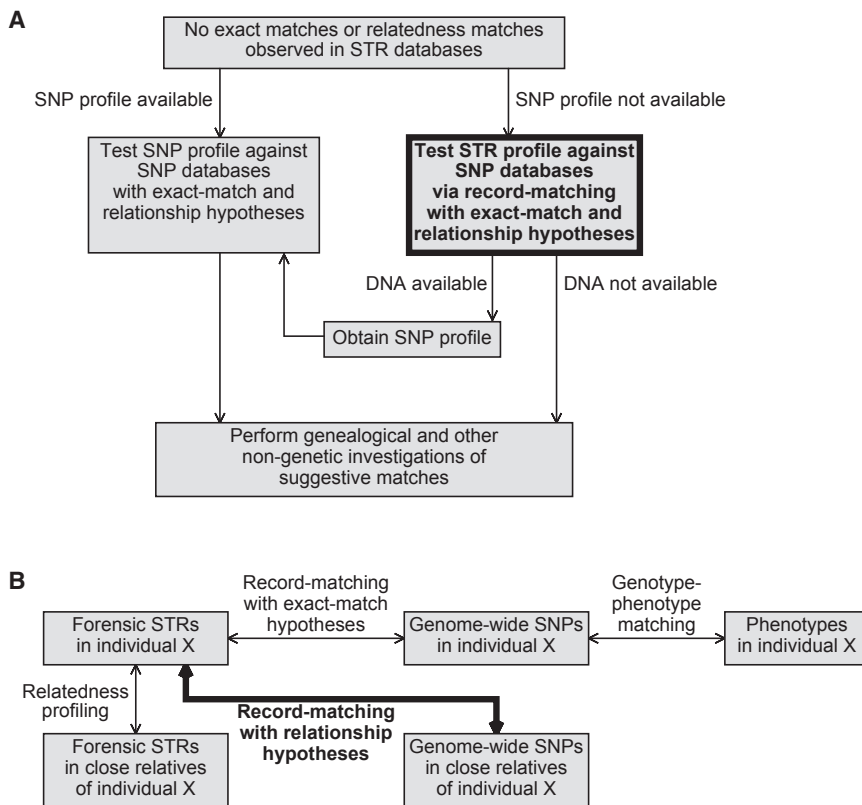
A

B

analyzed record-matching accuracy by geographic region of origin of the individuals. Although the effect of geographic ancestry on record-matching in the same-individual scheme was limited, owing to similar effects of ancestry on match scores for true matches and non-matching individuals (Edge et al., 2017), relatedness profiling has been seen to produce varying accuracy by population (Rohlfs et al., 2012, 2013) and might do so in record-matching as well.

The performance of the method will likely decrease with larger test sets that number in the thousands or millions. In large samples, the method will benefit from increased accuracy in inferring the LD pattern in the training set. However, larger test sets will reduce accuracy by generating larger numbers of possible matches. Accuracy improvements might be possible through the use of complete DNA sequence surrounding STRs, permitting improved phasing or prioritization in imputation of specific SNPs that have the highest LD with the STRs. In addition, although we have emphasized parent-offspring and sib-pair relationships, our mathematical framework permits computations with arbitrary relationship hypotheses more generally. For example, in Figure S1, we illustrate the use of test hypotheses across a grid of possible values to identify the value for Δ_{test} that generates the highest match score for a specific SNP profile and STR profile; thus, in principle, relationships between profiles could first be estimated and match accuracies then computed with estimated relationships. Attention to ancestry information in relationship estimation—as well as in phasing and imputation—can potentially improve inference in these steps (Conrad et al., 2006; Huang et al., 2009; Li et al., 2009; Manichaikul et al., 2010; Thornton et al., 2012; Moltke and Albrechtsen, 2014; Conomos et al., 2016), providing further opportunities to increase record-matching accuracy. Indeed, an analysis separating individuals by geographic region for pedigree construction, using region-specific allele frequencies in match-score calculations, and restricting attention to region-specific candidate matches (Table S3) suggests higher match accuracies than are seen in corresponding calculations that do not consider ancestry (Table 2).

of that relative—possibly through record-matching between phenotypes and SNP genotypes (Broman et al., 2015; Humbert et al., 2015). Thus, with access to SNP databases, the information contained in a CODIS profile would extend far beyond its value for the identification of its contributor to also include genome-wide genetic data and phenotypic information about relatives of that contributor (Figure 5B).

The possibility of performing familial searching of forensic profiles in SNP databases, while raising new concerns, also alters an existing concern, namely the unequal representation of populations in forensic databases. In profile queries to search for a relative already in a forensic database, populations overrepresented in databases owing to overrepresentation in criminal justice systems are likely to produce more identifications, potentially contributing to further overrepresentation (Greely et al., 2006; Chow-White and Duster, 2011; Rohlfs et al., 2013). Record-matching queries to biomedical, genealogical, or personal-genomic databases, however, will instead produce more identifications in different populations emphasized in genome-wide association and personal genomics (Chow-White and Duster, 2011; Popejoy and Fullerton, 2016; Landry et al., 2017).

We have focused only on identifying true relationship matches, and not on excluding pairs of STR and SNP profiles as potential matches. The indirectness of record-matching can lead to low match scores for some true relative pairs, as can misspecification of the relationship hypothesis; thus, a low match score might not reliably exclude a pair as relatives. We also have not

For record-matching of SNP and STR profiles with more distant relationships than in the parent-offspring and sib-pair cases, accuracy will be lower in the same manner that it is reduced for parent-offspring and sib-pair schemes compared to the case of matching profiles from the same individual. Nevertheless, this study contributes to growing understanding of the extent of the information contained in individual genotype profiles when those genotypes are analyzed together with databases of genotypes of other individuals, finding that that information can be considerable, both about the individuals typed and about their close relatives.

STAR★METHODS

Detailed methods are provided in the online version of this paper and include the following:

- KEY RESOURCES TABLE
- CONTACT FOR REAGENT AND RESOURCE SHARING
- EXPERIMENTAL MODEL AND SUBJECT DETAILS
- METHOD DETAILS
  - BEAGLE Settings
  - Pedigree Generation
  - Training and Test Sets
  - Additional STRs
- QUANTIFICATION AND STATISTICAL ANALYSIS
  - Overview of Match Score Calculation
  - Individual B is Heterozygous: $a_r \neq a_t$
  - Individual B is Homozygous: $a_r = a_t$
  - Completing the Calculation

AUTHOR CONTRIBUTIONS

Conceptualization, J.K., M.D.E., B.F.B.A.-H., J.Z.L., and N.A.R.; Project Design, J.K., M.D.E., and N.A.R.; Mathematical Theory, J.K., M.D.E., and N.A.R.; Simulations, J.K.; Data Analysis, J.K., M.D.E., and N.A.R.; Supervision, N.A.R.; Writing, all authors.

DECLARATION OF INTERESTS

The authors declare no competing interests.

REFERENCES

Bieber, F.R., Brenner, C.H., and Lazer, D. (2006). Human genetics. Finding criminals through DNA of their relatives. Science *312*, 1315–1316.

Broman, K.W., Keller, M.P., Broman, A.T., Kendziorski, C., Yandell, B.S., Sen, Ś., and Attie, A.D. (2015). Identification and correction of sample mix-ups in expression genetic data: a case study. G3 (Bethesda) *5*, 2177–2186.

Browning, S.R., and Browning, B.L. (2007). Rapid and accurate haplotype phasing and missing-data inference for whole-genome association studies by use of localized haplotype clustering. Am. J. Hum. Genet. *81*, 1084–1097.

Browning, B.L., and Browning, S.R. (2016). Genotype imputation with millions of reference samples. Am. J. Hum. Genet. *98*, 116–126.

Budowle, B., Shea, B., Niezgoda, S., and Chakraborty, R. (2001). CODIS STR loci data from 41 sample populations. J. Forensic Sci. *46*, 453–489.

Butler, J.M. (2006). Genetics and genomics of core short tandem repeat loci used in human identity testing. J. Forensic Sci. *51*, 253–265.

Butler, J.M. (2012). Advanced Topics in Forensic DNA Typing: Methodology (San Diego: Elsevier Academic Press).

Chow-White, P.A., and Duster, T. (2011). Do health and forensic DNA databases increase racial disparities? PLoS Med. *8*, e1001100.

Conomos, M.P., Reiner, A.P., Weir, B.S., and Thornton, T.A. (2016). Model-free estimation of recent genetic relatedness. Am. J. Hum. Genet. *98*, 127–148.

Conrad, D.F., Jakobsson, M., Coop, G., Wen, X., Wall, J.D., Rosenberg, N.A., and Pritchard, J.K. (2006). A worldwide survey of haplotype variation and linkage disequilibrium in the human genome. Nat. Genet. *38*, 1251–1260.

Curran, J.M., and Buckleton, J.S. (2008). Effectiveness of familial searches. Sci. Justice *48*, 164–167.

Dou, J., Sun, B., Sim, X., Hughes, J.D., Reilly, D.F., Tai, E.S., Liu, J., and Wang, C. (2017). Estimation of kinship coefficient in structured and admixed populations using sparse sequencing data. PLoS Genet. *13*, e1007021.

Edge, M.D., Algee-Hewitt, B.F.B., Pemberton, T.J., Li, J.Z., and Rosenberg, N.A. (2017). Linkage disequilibrium matches forensic genetic records to disjoint genomic marker sets. Proc. Natl. Acad. Sci. USA *114*, 5671–5676.

Gershaw, C.J., Schweighardt, A.J., Rourke, L.C., and Wallace, M.M. (2011). Forensic utilization of familial searches in DNA databases. Forensic Sci. Int. Genet. *5*, 16–20.

Greely, H.T., and Kaye, D.H. (2013). A brief of genetics, genomics and forensic science researchers in Maryland v. King. Jurimetrics *54*, 43–64.

Greely, H.T., Riordan, D.P., Garrison, N.A., and Mountain, J.L. (2006). Family ties: the use of DNA offender databases to catch offenders' kin. J. Law Med. Ethics *34*, 248–262.

Hares, D.R. (2015). Selection and implementation of expanded CODIS core loci in the United States. Forensic Sci. Int. Genet. *17*, 33–34.

Huang, L., Li, Y., Singleton, A.B., Hardy, J.A., Abecasis, G., Rosenberg, N.A., and Scheet, P. (2009). Genotype-imputation accuracy across worldwide human populations. Am. J. Hum. Genet. *84*, 235–250.

Humbert, M., Huguenin, K., Hugonot, J., Ayday, E., and Hubaux, J.P. (2015). De-anonymizing genomic databases using phenotypic traits. PoPETs *2015*, 99–114.

Jacquard, A. (1972). Genetic information given by a relative. Biometrics *28*, 1101–1114.

Katsanis, S.H., and Wagner, J.K. (2013). Characterization of the standard and recommended CODIS markers. J. Forensic Sci. *58* (*Suppl 1*), S169–S172.

Kuhn, H.W. (1955). The Hungarian method for the assignment problem. NRL *2*, 83–97.

Kuhn, J.M.M., Jakobsson, M., and Günther, T. (2018). Estimating genetic kin relationships in prehistoric populations. PLoS ONE *13*, e0195491.

Landry, L., Nielsen, D.E., Carere, D.A., Roberts, J.S., and Green, R.C.; PGen Study Group (2017). Racial minority group interest in direct-to-consumer genetic testing: findings from the PGen study. J. Community Genet. *8*, 293–301.

Lange, K. (1997). Mathematical and Statistical Methods for Genetic Analysis (New York: Springer).

Li, Y., Willer, C., Sanna, S., and Abecasis, G. (2009). Genotype imputation. Annu. Rev. Genomics Hum. Genet. *10*, 387–406.

Manichaikul, A., Mychaleckyj, J.C., Rich, S.S., Daly, K., Sale, M., and Chen, W.M. (2010). Robust relationship inference in genome-wide association studies. Bioinformatics 26, 2867–2873.

Martin, M.D., Jay, F., Castellano, S., and Slatkin, M. (2017). Determination of genetic relatedness from low-coverage human genome sequences using pedigree simulations. Mol. Ecol. 26, 4145–4157.

Moltke, I., and Albrechtsen, A. (2014). RelateAdmix: a software tool for estimating relatedness between admixed individuals. Bioinformatics 30, 1027–1028.

Murphy, E. (2010). Relative doubt: familial searches of DNA databases. Mich. Law Rev. 109, 291–348.

Popejoy, A.B., and Fullerton, S.M. (2016). Genomics is failing on diversity. Nature 538, 161–164.

Rohlfs, R.V., Fullerton, S.M., and Weir, B.S. (2012). Familial identification: population structure and relationship distinguishability. PLoS Genet. 8, e1002469.

Rohlfs, R.V., Murphy, E., Song, Y.S., and Slatkin, M. (2013). The influence of relatives on the efficiency and error rate of familial searching. PLoS ONE 8, e70495.

Snyder-Mackler, N., Majoros, W.H., Yuan, M.L., Shaver, A.O., Gordon, J.B., Kopp, G.H., Schlebusch, S.A., Wall, J.D., Alberts, S.C., Mukherjee, S., et al. (2016). Efficient genome-wide sequencing and low-coverage pedigree analysis from noninvasively collected samples. Genetics 203, 699–714.

Theunert, C., Racimo, F., and Slatkin, M. (2017). Joint estimation of relatedness coefficients and allele frequencies from ancient samples. Genetics 206, 1025–1035.

Thompson, E.A. (1976). A restriction on the space of genetic relationships. Ann. Hum. Genet. 40, 201–204.

Thornton, T., Tang, H., Hoffmann, T.J., Ochs-Balcom, H.M., Caan, B.J., and Risch, N. (2012). Estimating kinship in admixed populations. Am. J. Hum. Genet. 91, 122–138.

United States Supreme Court. (2013). Maryland v King, 133 S. Ct. 1958.

Vohr, S.H., Buen Abad Najar, C.F., Shapiro, B., and Green, R.E. (2015). A method for positive forensic identification of samples from extremely low-coverage sequence data. BMC Genomics 16, 1034.

STAR★METHODS

KEY RESOURCES TABLE

REAGENT or RESOURCE	SOURCE	IDENTIFIER
Software and Algorithms		
BEAGLE 4.1	Browning and Browning, 2007, 2016	https://faculty.washington.edu/browning/beagle/b4_1.html
Custom computer code	This paper	Available from the Lead Contact upon request
Other		
Genotype data	Edge et al., 2017	http://rosenberglab.stanford.edu/diversity.html

CONTACT FOR REAGENT AND RESOURCE SHARING

Further information and requests for resources, including computer code implementing the mathematical formulas used in this study, should be directed to and will be fulfilled by the lead contact, Noah A. Rosenberg (noahr@stanford.edu).

EXPERIMENTAL MODEL AND SUBJECT DETAILS

The data consisted of diploid genotypes of 872 individuals typed for 642,563 autosomal SNP loci, 13 autosomal STR loci from the CODIS panel, 431 additional autosomal tetranucleotide STR loci and 1 trinuclotide locus, D22S1045, which appeared in the 2017 CODIS update (Hares, 2015). We used the same datasets as Edge et al. (2017), representing 52 worldwide populations in the Human Genome Diversity Panel, and containing no pairs of close relatives. Geographic regions and associated sample sizes followed Edge et al. (2017) (Africa, 76; Europe, 151; Middle East, 155; Central/South Asia, 198; East Asia, 227; Oceania, 26; America, 39).

METHOD DETAILS

BEAGLE Settings

Inference of haplotype phase and imputation of STR genotypes were performed using BEAGLE v4.1 (Browning and Browning, 2007, 2016). For each STR marker, we considered in BEAGLE 1-Mb SNP windows extending 500 kb in each direction from the STR midpoint.

For phasing, which we performed in two different steps—one prior to pedigree generation, and another for phasing training sets—we used the default number of 10 iterations in BEAGLE, and we used default BEAGLE phasing parameters: maxlr = 5,000, lowmem = false, window = 50,000, overlap = 3,000, impute = true, cluster = 0.005, ne = 1 million, err = 0.0001, seed = −99,999, and models-cale = 0.8.

We also used BEAGLE for imputation in test sets using phased training sets as reference data, employing a linkage map based on GRCh36 coordinates and the same parameters as in phasing, except gprobs = true and maxlr = 1 million.

Pedigree Generation

Prior to generating pedigrees, we first phased the entire dataset ("BEAGLE Settings") to obtain individual haplotypes for use in pedigree generation. Next, we chose pairs of individuals without replacement to obtain 436 parental pairs from the 872 sampled individuals. For each parental pair, we simulated two offspring. Assuming a 1 cM/Mb recombination rate, recombination would be expected to affect 1% of meioses when considering 1-Mb windows; for simplicity, we assumed that our 1-Mb window size was small enough that no recombination occurred within windows, so that these 1% of meioses produced haplotypes transmitted intact in nuclear pedigrees. STR loci were treated as independent, so that assortment was independent across STRs.

Once pedigrees were generated, we dephased haplotypes, randomizing allele orders within individuals to hide phase information. We generated 10 sets of random pedigrees, each containing a distinct pairing of the 872 individuals into parental pairs. We used the same 10 sets in the parent–offspring and sib-pair schemes.

Training and Test Sets

Following Edge et al. (2017), we partitioned our dataset into a training set with 75% of the individuals and a test set of size 25%. For our "same individuals" computations, 654 of 872 individuals were assigned to the training set, and the other 218 to the test set. For

these computations, we generated 100 random training–test partitions. We then imputed STR genotypes in the test set with the training set as a reference ("BEAGLE Settings"), constructing a 218×218 match-score matrix to match imputed STR genotypes in the test set to actual test-set STR genotypes.

For the parent–offspring scheme, without loss of generality, we placed parent genotypes in the SNP dataset and offspring genotypes in the STR dataset. For each of the 10 sets of random pedigrees, we generated 10 random partitions into training and test sets, for a total of 100 training–test partitions. Each partition contained a training set of 75% of the pedigrees (327 pedigrees) and a test set with the other 25% (109 pedigrees). For each partition, we phased the training set ("BEAGLE Settings"), including only the 654 parental individuals in the computation, to produce a phased reference panel. To produce a test set, from each test-set pedigree, we chose one parent and one offspring, creating 109 parent–offspring pairs. We then imputed STR genotypes of parents in the test set with the training set as a reference ("BEAGLE Settings") and constructed a 109×109 match-score matrix to match the imputed STR genotypes of parents in the test set to STR genotypes of offspring in the test set.

For the sib-pair scheme, as in the parent–offspring scheme, we generated 10 random partitions of each of the 10 sets of random pedigrees to produce 100 training–test partitions. For each partition, we assigned 75% of the pedigrees to the training set and 25% to the test set. Next, we took the parents from each training-set pedigree to form a training set that we then phased ("BEAGLE Settings"). For a test set, a set of 109 siblings, each randomly selected from a pedigree, was used for the SNP dataset, and the remaining 109 siblings acted as an STR dataset. We imputed STR genotypes of the sibs in the test set with the training set as a reference ("BEAGLE Settings") and constructed a 109×109 match-score matrix to match the imputed STR genotypes in the half of the sibs treated as having SNP data in the test set to the STR genotypes of the other half of the sibs in the test set.

Allele frequencies for match score computations were obtained from the training set for the exact-match calculations, and from the parents in the training set for the parent–offspring and sib-pair calculations. In selecting median-accuracy partitions, we chose the lesser of two possible median values among 100 partitions.

Additional STRs

We scanned numbers of loci from 5 to 100 with an increment of 5. From 431 non-CODIS tetranucleotide STR loci, we initially generated 100 sets of 100 random loci. For each set of loci, we recursively selected subsequent sets of loci with fewer loci at random so that the newly selected set of loci was nested in the previous set.

For each of the three true relationships (same individual, parent–offspring, sib pairs), we selected a partition and a pedigree set corresponding to the median one-to-one record-matching accuracy in the case of $\Delta_{\text{true}} = \Delta_{\text{test}}$ (Figures 2A, 2E, and 2I). We then ran our record-matching computations for each of the 100 sets of non-CODIS STR loci, considering each of the three test hypotheses (same individual, parent–offspring, sib pairs) and each of the four match-assignment scenarios (one-to-one, one-to-many with SNP query, one-to-many with STR query, needle-in-haystack).

QUANTIFICATION AND STATISTICAL ANALYSIS

Overview of Match Score Calculation

To calculate the match score of Equation 1 under an arbitrary relatedness hypothesis Δ, we must calculate the probability of STR profile R_A given SNP profile S_B and the relatedness hypothesis $M = \Delta$ for individuals A and B, $\mathbb{P}(R_A \mid S_B, M = \Delta)$, and the unconditional probability of R_A, $\mathbb{P}(R_A)$.

Assuming independence of STR loci, the probabilities of STR profiles are obtained as products across loci,

$$\mathbb{P}(R_A \mid S_B, M = \Delta) = \prod_{\ell=1}^{L} \mathbb{P}(R_{A\ell} \mid S_{B\ell}, M = \Delta) \tag{3}$$

$$\mathbb{P}(R_A) = \prod_{\ell=1}^{L} \mathbb{P}(R_{A\ell}). \tag{4}$$

$\mathbb{P}(R_{A\ell})$ is calculated as the Hardy-Weinberg frequency of genotypes at locus ℓ.

To evaluate $\mathbb{P}(R_{A\ell} \mid S_{B\ell}, \Delta)$ in Equation 3, the probability for an individual A to have STR genotype $R_{A\ell}$ at locus ℓ, conditional on a relative B having SNP genotype $S_{B\ell}$ and relationship $\Delta = (\Delta_0, \Delta_1, \Delta_2)$, we sum over all values of $R_{B\ell}$ in $\mathscr{R}_\ell$, the set of all possible unordered diploid genotypes at STR locus ℓ:

$$\mathbb{P}(R_{A\ell} \mid S_{B\ell}, \Delta) = \sum_{R_{B\ell} \in \mathscr{R}_\ell} \mathbb{P}(R_{A\ell} \mid R_{B\ell}, \Delta) \mathbb{P}(R_{B\ell} \mid S_{B\ell}). \tag{5}$$

$\mathbb{P}(R_{B\ell} \mid S_{B\ell}, \Delta = (0,0,1))$, or $\mathbb{P}(R_{B\ell} \mid S_{B\ell})$ for short, is the probability for an individual B with SNP genotype $S_{B\ell}$ at locus ℓ to have STR genotype $R_{B\ell}$ at locus ℓ. We used BEAGLE to estimate the imputation probability for STR genotype $R_{B\ell}$ given surrounding SNP profile $S_{B\ell}$ in the same individual (see "BEAGLE Settings").

To obtain $\mathbb{P}(R_{A\ell} \mid R_{B\ell}, \Delta)$ for arbitrary Δ, we denote the unordered STR genotypes of individuals A and B at locus ℓ by $R_{A\ell} = a_m a_n$ and $R_{B\ell} = a_r a_t$, respectively. Alleles a_m, a_n, a_r, and a_t have allele frequencies p_m, p_n, p_r, and p_t, respectively, and they are not necessarily distinct. We decompose $\mathbb{P}(R_{A\ell} \mid R_{B\ell}, \Delta)$ by conditioning on all possible identity states C_k describing the pair of individuals A and B (Table 1):

$$\mathbb{P}(R_{A\ell} = a_m a_n \mid R_{B\ell} = a_r a_t, \Delta) = \sum_{k=0}^{2} \mathbb{P}(R_{A\ell} = a_m a_n \mid C_k, R_{B\ell} = a_r a_t)\, \mathbb{P}(C_k \mid R_{B\ell} = a_r a_t, \Delta). \tag{6}$$

To evaluate the summands, we consider two separate cases: (1) individual B is heterozygous, and (2) individual B is homozygous. In each case, we assume Hardy-Weinberg genotype frequencies at locus ℓ.

Individual B is Heterozygous: $a_r \neq a_t$

Using the joint probability distribution of C_k and the genotype of the individual B (Table 1), a state C_k has probability:

$$\mathbb{P}(C_k \mid R_{B\ell} = a_r a_t, \Delta) = \frac{\mathbb{P}(C_k, R_{B\ell} = a_r a_t \mid \Delta)}{\mathbb{P}(R_{B\ell} = a_r a_t \mid \Delta)} = \frac{2 p_r p_t \Delta_k}{2 p_r p_t} = \Delta_k. \tag{7}$$

To evaluate Equation 6, it remains to compute $\mathbb{P}(R_{A\ell} \mid C_k, R_{B\ell} = a_r a_t)$ for each identity state C_k, $k = 0, 1, 2$. For the remainder of the case of B heterozygous, we treat m, n, r, and t as distinct.

C_0: No alleles in A are identical by descent (IBD) with an allele in B. Hence, genotype probabilities in A follow Hardy-Weinberg frequencies:

$$\mathbb{P}(R_{A\ell} \mid C_0, R_{B\ell} = a_r a_t) = \begin{cases} p_r^2 & R_{A\ell} = a_r a_r \\ p_t^2 & R_{A\ell} = a_t a_t \\ p_m^2 & R_{A\ell} = a_m a_m \\ 2 p_r p_t & R_{A\ell} = a_r a_t \\ 2 p_r p_m & R_{A\ell} = a_r a_m \\ 2 p_t p_m & R_{A\ell} = a_t a_m \\ 2 p_m p_n & R_{A\ell} = a_m a_n. \end{cases} \tag{8}$$

C_1: The only identity-by-descent relationship is between one allele of A and one allele of B. Thus, A can have genotype either $a_r a_v$ or $a_t a_v$, where a_v can be any allele in the population. Because a_r and a_t have the same probability of being the allele of B that is IBD with an allele in A, we have:

$$\mathbb{P}(R_{A\ell} \mid C_1, R_{B\ell} = a_r a_t) = \begin{cases} \dfrac{1}{2} p_r & R_{A\ell} = a_r a_r \\[2mm] \dfrac{1}{2} p_t & R_{A\ell} = a_t a_t \\[2mm] \dfrac{1}{2} p_r + \dfrac{1}{2} p_t & R_{A\ell} = a_r a_t \\[2mm] \dfrac{1}{2} p_m & R_{A\ell} = a_r a_m \\[2mm] \dfrac{1}{2} p_m & R_{A\ell} = a_t a_m \\[2mm] 0 & \text{otherwise.} \end{cases} \tag{9}$$

C_2: One allele of A is IBD with one allele from B, and the other allele from A is IBD with the other allele from B. Thus, A and B have the same unordered genotype: $a_m a_n = a_r a_t$:

$$\mathbb{P}(R_{A\ell} \mid C_2, R_{B\ell} = a_r a_t) = \begin{cases} 1 & R_{A\ell} = a_r a_t \\ 0 & \text{otherwise.} \end{cases} \tag{10}$$

Combining Equations 7, 8, 9, and 10, for heterozygous $R_{B\ell}$, with r, t, m, and n all distinct and $R_{B\ell} = a_r a_t$, we have:

$$\mathbb{P}(R_{A\ell} \mid R_{B\ell} = a_r a_t, \boldsymbol{\Delta}) = \begin{matrix} \Delta_0 & \Delta_1 & \Delta_2 & R_{A\ell} \\ \begin{bmatrix} p_r^2 \Delta_0 & +\frac{1}{2}p_r \Delta_1 & & \\ p_t^2 \Delta_0 & +\frac{1}{2}p_t \Delta_1 & & \\ p_m^2 \Delta_0 & & & \\ 2p_r p_t \Delta_0 & +(\frac{1}{2}p_r + \frac{1}{2}p_t)\Delta_1 & +\Delta_2 & \\ 2p_r p_m \Delta_0 & +\frac{1}{2}p_m \Delta_1 & & \\ 2p_t p_m \Delta_0 & +\frac{1}{2}p_m \Delta_1 & & \\ 2p_m p_n \Delta_0 & & & \end{bmatrix} & & & \begin{matrix} a_r a_r \\ a_t a_t \\ a_m a_m \\ a_r a_t \\ a_r a_m \\ a_t a_m \\ a_m a_n. \end{matrix} \end{matrix}$$

(11)

In this matrix notation, each row represents a probability for a particular choice of $R_{A\ell}$, summing across cases $\boldsymbol{C}_0$, $\boldsymbol{C}_1$, and $\boldsymbol{C}_2$. The distinct alleles a_m and a_n refer to alleles different from a_r and a_t. We use notation $T_{rt}(x, y)$ to represent the quantity associated with $R_{A\ell} = a_x a_y$ in Equation 11.

Individual B is Homozygous: $a_r = a_t$

When B is homozygous with genotype $a_r a_r$, using Table 1, the identity state C_k has probability:

$$\mathbb{P}(C_k \mid R_{B\ell} = a_r a_r, \boldsymbol{\Delta}) = \frac{\mathbb{P}(C_k, R_{B\ell} = a_r a_r \mid \boldsymbol{\Delta})}{\mathbb{P}(R_{B\ell} = a_r a_r \mid \boldsymbol{\Delta})} = \frac{p_r^2 \Delta_k}{p_r^2} = \Delta_k.$$

(12)

$\boldsymbol{C}_0$: None of the alleles are IBD, and A can have any possible genotype:

$$\mathbb{P}(R_{A\ell} \mid C_0, R_{B\ell} = a_r a_r) = \begin{cases} p_r^2 & R_{A\ell} = a_r a_r \\ p_m^2 & R_{A\ell} = a_m a_m \\ 2p_r p_m & R_{A\ell} = a_r a_m \\ 2p_m p_n & R_{A\ell} = a_m a_n. \end{cases}$$

(13)

$\boldsymbol{C}_1$: One allele of A is IBD with one allele of B, and remaining alleles of A and B have no identity by descent. Because B is homozygous with genotype $a_r a_r$, A has genotype $a_r a_v$, where a_v is any possible allele:

$$\mathbb{P}(R_{A\ell} \mid C_1, R_{B\ell} = a_r a_r) = \begin{cases} p_r & R_{A\ell} = a_r a_r \\ p_m & R_{A\ell} = a_r a_m \\ 0 & \text{otherwise.} \end{cases}$$

(14)

$\boldsymbol{C}_2$: One allele in A is IBD with one allele in B, and the other allele in A is IBD with the other allele in B. A therefore has the same genotype as B:

$$\mathbb{P}(R_{A\ell} \mid C_2, R_{B\ell} = a_r a_r) = \begin{cases} 1 & R_{A\ell} = a_r a_r \\ 0 & \text{otherwise.} \end{cases}$$

(15)

Combining all cases, from Equations 12, 13, 14, and 15, with a_m, a_n, and a_r all distinct and $R_{B\ell} = a_r a_r$, we obtain:

$$\mathbb{P}(R_{A\ell} \mid R_{B\ell} = a_r a_r, \boldsymbol{\Delta}) = \begin{matrix} \Delta_0 & \Delta_1 & \Delta_2 & R_{A\ell} \\ \begin{bmatrix} p_r^2 \Delta_0 & +p_r \Delta_1 & +\Delta_2 & \\ p_m^2 \Delta_0 & & & \\ 2p_r p_m \Delta_0 & +p_m \Delta_1 & & \\ 2p_m p_n \Delta_0 & & & \end{bmatrix} & & & \begin{matrix} a_r a_r \\ a_m a_m \\ a_r a_m \\ a_m a_n. \end{matrix} \end{matrix}$$

(16)

Here, the alleles a_m and a_n are distinct and indicate any alleles different from a_r. We use notation $H_{rr}(x, y)$ to represent the quantity associated with $R_{A\ell} = a_x a_y$ in Equation 16.

Completing the Calculation

We can now expand Equation 3 for arbitrary relationships $M = \boldsymbol{\Delta}$. Let N_ℓ denote the number of distinct alleles possible at STR locus ℓ, and index these alleles by $\{a_1, a_2, \ldots, a_{N_\ell}\}$. From Equations 5, 11, and 16, recalling that $\mathbb{P}(R_{B\ell} \mid S_{B\ell})$ is obtained from BEAGLE, we have

$$
\begin{aligned}
\mathbb{P}(R_A \mid S_B, M = \boldsymbol{\Delta}) &= \prod_{\ell=1}^{L} \mathbb{P}(R_{A\ell} = a_{m_\ell} a_{n_\ell} \mid S_{B\ell}, \boldsymbol{\Delta}) \\
&= \prod_{\ell=1}^{L} \sum_{t_\ell=1}^{N_\ell} \sum_{r_\ell=1}^{t_\ell} \mathbb{P}(R_{B\ell} = a_{r_\ell} a_{t_\ell} \mid S_{B\ell}) \mathbb{P}(R_{A\ell} = a_{m_\ell} a_{n_\ell} \mid R_{B\ell} = a_{r_\ell} a_{t_\ell}, \boldsymbol{\Delta}) \\
&= \prod_{\ell=1}^{L} \sum_{t_\ell=1}^{N_\ell} \sum_{r_\ell=1}^{t_\ell} [\mathbb{P}(R_{B\ell} = a_{r_\ell} a_{t_\ell} \mid S_{B\ell})(T_{r_\ell t_\ell}(m_\ell, n_\ell)(1 - \delta_{r_\ell t_\ell}) + H_{r_\ell r_\ell}(m_\ell, n_\ell)\delta_{r_\ell t_\ell})].
\end{aligned}
$$
(17)

In the last step, we use the Kronecker delta to combine the heterozygous case of Equation 11 and the homozygous case of Equation 16 into a single equation.
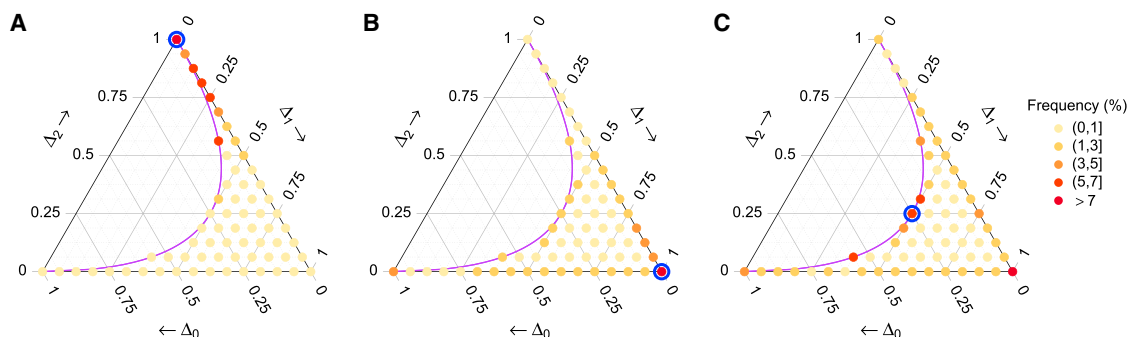
Figure S1. Choices of Δ_{test} that Produce the Highest Match Score in Comparisons of Genome-wide SNP and CODIS STR Profiles, Related to Table 2

We examined a grid of 65 hypotheses Δ_{test} in the Thompson (1976) region of points $(\Delta_0, \Delta_1, \Delta_2)$ that represent actual relationships between non-inbred pairs of individuals (right side of the curved line), considering a mesh of width $1/16$ for Δ_0, Δ_1, and Δ_2. For each of the 100 partitions studied in Table 2, for each of the 218 or 109 individuals in the test set (218 for exact-match, 109 for parent–offspring and sib pairs), we identified the hypothesized relationship Δ_{test} that maximized the match score. For each Δ_{true}, for each Δ_{test} value, the percentage of the 21,800 or 10,900 cases producing that Δ_{test} as the maximizing value is plotted. The location of Δ_{true} is marked in blue. (A) $\Delta_{\text{true}} = (0, 0, 1)$, same individual. (B) $\Delta_{\text{true}} = (0, 1, 0)$, parent–offspring. (C) $\Delta_{\text{true}} = (1/4, 1/2, 1/4)$, sib pairs. The single values of Δ_{test} that maximize the match score for more than 7% of cases do so for 50.8%, 28.6%, and 11.0% of cases in (A), (B), and (C), respectively. In (A) and (B), this value of Δ_{test} accords with Δ_{true}; in (C), it misspecifies sib pairs as parent–offspring pairs.